

See discussions, stats, and author profiles for this publication at: <https://www.researchgate.net/publication/6649258>

# Theoretical Study on Molecular Property of Protactinium(V) and Uranium(VI) Oxocations: Why Does Protactinium(V) Form Monooxo Cations in Aqueous Solution?

ARTICLE *in* THE JOURNAL OF PHYSICAL CHEMISTRY A · JANUARY 2007

Impact Factor: 2.69 · DOI: 10.1021/jp0641435 · Source: PubMed

---

CITATIONS

18

---

READS

40

3 AUTHORS, INCLUDING:



Takashi Toraishi

The University of Tokyo

16 PUBLICATIONS 256 CITATIONS

SEE PROFILE



Takao Tsuneda

University of Yamanashi

68 PUBLICATIONS 3,918 CITATIONS

SEE PROFILE

# Theoretical Study on Molecular Property of Protactinium(V) and Uranium(VI) Oxocations: Why Does Protactinium(V) Form Monooxo Cations in Aqueous Solution?

Takashi Toraishi,\* Takao Tsuneda, and Satoru Tanaka

Department of Quantum Engineering and Systems Science, Graduate School of Engineering, The University of Tokyo, Tokyo 113-8656, Japan

Received: July 2, 2006; In Final Form: September 3, 2006

The stability of Pa(V) and U(VI) oxocations in aqueous solution were theoretically investigated by means of density functional theory calculations. As a result, the present calculations clearly supported an experimental result from an energetic point of view that monooxo protactinyl cation,  $\text{PaO}^{3+}$ , is a preferable species for Pa(V) in aqueous solution, although dioxo protactinyl cation,  $\text{PaO}_2^+$ , is not a feasible form. By an analysis of molecular orbitals, we revealed that 6d orbitals of Pa(V) destabilize the  $\pi$  orbitals of  $\text{PaO}_2^+$ , because 6d-2p antibonding orbital conflicts with another 5f-2p bonding orbital. For stable dioxo uranyl cation,  $\text{UO}_2^{2+}$ , we found that 6d orbitals of U(VI), in contrast, form a bonding orbital with the 2p orbitals, and this bonding orbital coexists at an angle with the 5f-2p bonding orbital due to an electron correlation.

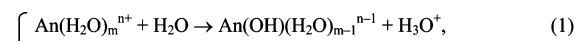
## 1. Introduction

Chemical properties of actinide elements strongly depend on the 5f/6d electronic configuration. Several actinides, including uranium, neptunium, plutonium, and americium, form dioxo “actinyl” ions,  $\text{AnO}_2^{x+}$  ( $x = 1$  or  $2$ ), which consist of two strong An–O triple bonds.<sup>1</sup> In contrast, the dioxo ion is less favored only for pentavalent protactinium Pa(V), which is the first actinide with 5f electrons involved in bonding. It is well-known that hexavalent uranium U(VI), which takes an isoelectric electron configuration with Pa(V), forms strong dioxo cation,  $\text{UO}_2^{2+}$ , in aqueous solution.<sup>2,3</sup> Also in the case of Np(V), which is the first stable form of pentavalent trans uranium elements, it is encountered as a dioxo cation  $\text{NpO}_2^+$ . Based on these analogues between Pa(V) and other actinides, it is natural to believe that Pa(V) dioxo cations are also the stable chemical species. In fact, in the early 1950s, the existence of  $\text{PaO}_2^+$  was postulated from cation exchange experiments.<sup>4</sup> However, it is known at present that only the monooxo species,  $\text{PaO}(\text{OH})_2^{2+}$  and  $\text{PaO}(\text{OH})_2^+$ , are the stable species in aqueous media. At tracer scale ( $\sim 10^{-12}$  M) and for freshly prepared solutions, Pa(V) in inorganic acid ( $\text{HClO}_4$ ,  $\text{HNO}_3$ ,  $\text{HCl}$ , or  $\text{H}_2\text{SO}_4$ ) exists under a mixture of oxo/hydroxo forms in equilibrium.<sup>5</sup> In acidic noncomplexing media ( $\text{HClO}_4$ ), the assumed species are  $\text{PaO}(\text{OH})_2^{2+}$ ,  $\text{PaO}(\text{OH})_2^+$ , and  $\text{Pa}(\text{OH})_5$ . Also in complexing media ( $\text{HCl}$  or  $\text{H}_2\text{SO}_4$ ), the presence of a Pa–O bond has been postulated from spectrophotometric measurements in the UV region.<sup>6</sup> Furthermore, very recently, Le Naour and co-workers first found the monooxo protactinium ion as a trissulfato complex,  $\text{PaO}(\text{SO}_4)_3^{3-}$ , in strong acidic media by means of X-ray absorption spectroscopy (XAS).<sup>7</sup> These data indicated that the monooxo species are the most feasible chemical speciation of pentavalent protactinium in aqueous solution. There are several reports on analogies between Pa(V) and group 5 elements (Nb and Ta) at the oxidation state V.<sup>8</sup> The occurrence of a monooxo cation has been proposed at oxidation state V, although the existing information on Nb and Ta species in

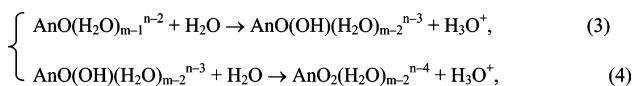
aqueous solution is scarce. Also in the solid state, it is well-known that a short Nb–O monooxo bond forms in the Nb(V) oxohalide series. However, these analogues do not consider the unique character of Pa(V), 5f orbitals in chemical bondings. Therefore, a theoretical approach is necessary for further investigation.

Pentavalent protoactinium Pa(V) plays a key role in the prediction of radiotoxic hazard from nuclear waste depository sites, since  $^{231}\text{Pa}$  ( $y^{1/2} = 3.28 \times 10^4$ ), which is produced through  $^{235}\text{U}$  decay chain ( $^{235}\text{U} \rightarrow \alpha \text{ } ^{231}\text{Th} \rightarrow \beta^- \text{ } ^{231}\text{Pa}$ ), is one of the key nuclei dominating radioactive toxicity in  $10^6$  years time period.<sup>9</sup> In aqueous solution, Pa(V) shows a strong tendency toward hydrolysis and polymerized colloid formation. This hydroxide colloid formation makes the prediction of its migration behavior in underground water systems complicated. Therefore, the detailed chemical knowledge has been sought for understanding those complicate chemical behaviors. Nevertheless, very few chemical information of Pa(V) is available in this stage. So far, as mentioned above, even the reason for the unique monooxo speciation of Pa(V) is still unknown, and no experimental approach can answer this question. In this study, we, therefore, investigate the stability of monooxo protactinium ion by means of density functional theory (DFT) calculations in comparison to mono- and dioxo isoelectric hexavalent uranums. We will theoretically illustrate the mechanism of Pa(V) monooxo cation formation, which will give a helpful information on the characteristic chemical behavior of Pa(V) in solution.

Now, we assume the following elemental reactions for the mono- and dioxo ion formations for simplicity: For monooxo cation formation



and for dioxo cation formation



\* Corresponding author phone: +81-3-5841-6970; fax: +81-3-3818-3455; e-mail: toraishi.takashi@jaea.go.jp. Present address: Research Group for Actinide Separation Chemistry, Japan Atomic Energy Agency (JAEA), Tokai-Mura, Ibaraki, 319-1195, Japan.

where An denotes pentavalent protactinium (Pa(V)) or hexavalent uranium (U(VI)),  $m$  is the number of coordination waters, and  $n$  is the formal valency of the central metal ion. Experimental data suggested that the major difference between Pa(V) and U(VI) is in the second step of the dioxo cation formation reactions, formula 4. In the Pa(V) system, reaction 4 never proceeds, although this is a spontaneous reaction for U(VI) in solution. In the present work, we first obtain the reaction energies of formulas 1–4 by means of DFT calculations to confirm that the dioxo cation formation is energetically less favored than the monooxo one for pentavalent protactinium. We note that the value  $m$  is set at seven in the present study, since the hydration number of the dioxo actinide cations ( $m-2$ ) is known at five. Next, the electronic structures and An–O bonding properties of mono- and dioxo cations of Pa(V) and U(VI) species were compared to reveal the instability of  $\text{PaO}_2^{2+}$  species. In this procedure, the Kohn–Sham orbitals of their bare ions, which hereafter indicate  $\text{PaO}_x$  or  $\text{UO}_x$  species with no explicit water molecules, were compared instead of those with coordination waters to emphasize the difference of their characteristics.

## 2. Calculations

Energy calculations and geometry optimizations were carried out for hydrated systems (cf. eqs 1–4) using B3LYP on Gaussian 03 program.<sup>10–12</sup> The availability of calculated B3LYP energies has been confirmed for actinide systems in another study.<sup>13</sup> The hydration effect was taken into account by means of Conductor-like Polarizable Continuum Model (CPCM) formulation with a parameter of  $\epsilon = 78.39$ .<sup>14</sup> The reaction energies of the formulas 1–4 were investigated on calculated CPCM single-point energies with the optimized geometries in gas phase. For bare ion calculations, we used Slater exchange + VWN correlation functional (SVWN),<sup>15,16</sup> Becke 1988 exchange + Lee–Yang–Parr exchange functional (BLYP),<sup>11,17</sup> B3LYP functional and a long-range corrected (LC) functional.<sup>18</sup> This is because we found a considerable functional-dependence in the constituent atomic orbitals of calculated Kohn–Sham orbitals, although no differences were given in the molecular structures and reaction energies (vide infra). In the LC scheme, we used Becke 1988 exchange + one-parameter progressive correlation (BOP) functional.<sup>17,19</sup> All calculations of bare ion systems were performed on GAMESS program<sup>20</sup> because of the numerical integration failure on Gaussian 03. For Pa and U, we used an energy-adjusted quasi-relativistic small-core pseudopotential with 60 core electrons with the corresponding valence basis sets suggested by Dolg et al.<sup>21</sup> plus two diffuse  $g$  functions. The Stuttgart-type quasi-relativistic pseudopotential with the corresponding valence basis set and Huzinaga basis sets were used for O and H, respectively, in calculations of hydrated systems.<sup>22,23</sup> In the calculations of bare ion systems, cc-pVTZ basis set was employed for O and H.<sup>24</sup> No symmetry was imposed for the hydrated components. We set  $C_{2v}$  symmetry for  $\text{Pa}(\text{H}_2\text{O})_5^{5+}$ ,  $\text{PaOH}^{4+}$ ,  $\text{PaO}(\text{H}_2\text{O})_3^{3+}$ ,  $\text{PaO}^{3+}$ ,  $\text{PaO}(\text{OH})_2^{2+}$ ,  $\text{U}(\text{H}_2\text{O})_6^{6+}$ ,  $\text{UOH}^{5+}$ ,  $\text{UO}(\text{H}_2\text{O})_4^{4+}$ , and  $\text{UO}(\text{OH})_3^{3+}$ , while no symmetry was forced to  $\text{PaO}_2^{2+}$  or  $\text{UO}_2^{2+}$  for the detailed discussion on their chemical bonds. The spin–orbit effect was not taken into account, because it is expected to be negligible due to the closed-shell structures of Pa(V) and U(VI). The shapes of coordination geometries and Kohn–Sham orbitals were drawn on MacMolPlot v.5.5.<sup>25</sup>

## 3. Results and Discussion

**Reliability of Present Calculation Models.** Now we examine the reliability of the coordination geometries of the present

**TABLE 1: Calculated Reaction Heat Energies (kJ/mol) of Formulas 1–4<sup>a</sup>**

	reaction			
	(1)	(2)	(3)	(4)
Pa(V)	−157.09	−52.19	−15.00	+111.36
U(VI)	−395.04	−203.20	−189.27	−99.94

<sup>a</sup> Energy values are electronic energies of reaction. In Kohn–Sham calculations, B3LYP functional was used with single-point CPCM. Positive heat energies denote endothermic and negative energies exothermic.

models. As mentioned above, it has been experimentally suggested that pentacoordinate aquo ions are formed for linear  $\text{UO}_2^{2+}$  cation and other trans-uranium dioxo cations,  $\text{NpO}_2^{2+}$  and  $\text{PuO}_2^{2+}$ .<sup>26</sup> Hence, it is reasonable to suppose that pentahydrated cation,  $\text{PaO}_2(\text{H}_2\text{O})_5^{3+}$ , is also a feasible coordination structure of Pa(V). For monooxo hydroxo cations, there is no experimental evidence for the number of coordination waters. However, the present calculations showed that the most stable OH- coordination site on bare  $\text{PaO}^{3+}$  and  $\text{UO}^{4+}$  cations are the trans-position of O (vide infra). Therefore, we suppose that the most feasible structure of  $\text{PaO}(\text{OH})_2^{2+}$  and  $\text{UO}(\text{OH})_3^{3+}$  is the linear structures with hydrated waters coordinating on these equatorial planes.

For monooxo aquo ions,  $\text{PaO}(\text{H}_2\text{O})_6^{3+}$  and  $\text{UO}(\text{H}_2\text{O})_6^{4+}$ , it is possible to take more than six coordination waters in these first hydration spheres. As a trial, we carried out geometry optimizations with attaching one coordinated water molecule on hexa-hydrated cations. However, we found no stable structures for such complexes. In the process of optimizations, water molecule always moved out of the first coordination spheres, and finally stayed in the second coordination spheres. We, therefore, considered that  $\text{PaO}(\text{H}_2\text{O})_6^{3+}$  and  $\text{UO}(\text{H}_2\text{O})_6^{4+}$  are the most stable hydrated structures of PaO and UO. On the other hand, hydroxo aquo ions,  $\text{PaOH}(\text{H}_2\text{O})_6^{4+}$  and  $\text{UOH}(\text{H}_2\text{O})_6^{5+}$ , and aquo ions,  $\text{Pa}(\text{H}_2\text{O})_7^{5+}$  and  $\text{U}(\text{H}_2\text{O})_7^{6+}$ , may have more hydration waters in the first hydration spheres. However, we suppose that this may not cause some problems in the present calculations, because the reaction heat energies of the formulas 1 and 2 (cf. Table 1) are sufficiently large in comparison with other paths for producing monooxo and dioxo cations. Although, for example, Tsushima et al. theoretically found that the most stable hydration number of Th(IV) aquo ion is ten,<sup>27</sup> the stabilized energies from 9–10 hydrations were calculated within 0.23 kJ/mol. This level of energy difference may not affect the conclusion from the present calculation.

**Stability of Monooxo and Dioxo Pa(V) Complexes.** In Table 1, the calculated energies of formulas 1–4 are summarized for Pa(V) and U(VI) cations in aqueous solution. Note that energy values in the table indicate electronic energies of reaction. The optimized geometries of Pa(V) species are also illustrated in Figure 1. The table clearly indicates that the dioxo cation formation of Pa(V) hardly proceeds in contrast to the formation of  $\text{UO}_2(\text{H}_2\text{O})_5^{2+}$  being a spontaneous reaction. The reaction energy of the formula (4) for Pa(V), +111.36 kJ/mol, is a quite contrast to that for U(VI), −99.94 kJ/mol. Recently, it was experimentally found that the dominant chemical species is not the dioxo but the monooxo hydroxo complex for Pa(V) in aqueous solution as is different from that for U(VI). The present result clearly supports this experimental finding. That is, the Pa(V) dioxo cation are energetically not favored in aqueous solution.

The optimized geometries and Mulliken atomic charges are displayed for mono- and dioxo complexes of Pa(V) and U(VI)

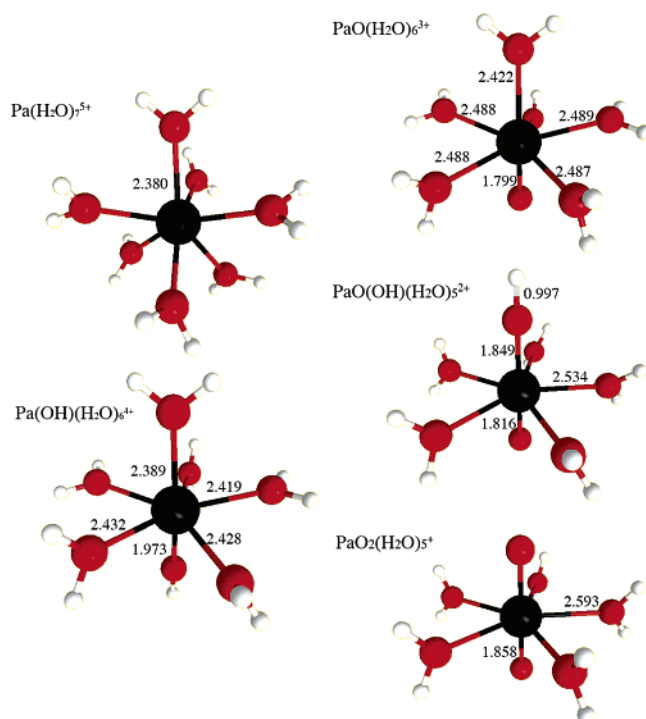


**Figure 1.** Optimized coordination geometries of  $\text{Pa}(\text{H}_2\text{O})_7^{5+}$ ,  $\text{Pa}(\text{OH})(\text{H}_2\text{O})_6^{4+}$ ,  $\text{PaO}(\text{H}_2\text{O})_6^{3+}$ ,  $\text{PaO}(\text{OH})(\text{H}_2\text{O})_5^{2+}$ , and  $\text{PaO}_2(\text{H}_2\text{O})_5^+$  in gas phase with several bond lengths in Å. B3LYP functional was used in Kohn–Sham calculations. Black, red, and white balls denote Pa, O, and H atoms, respectively.

in Table 2. This table also indicates that the instability of the dioxo Pa(V) cation is reflected in these properties. For all complexes, the bond length of Pa–O triple bond is longer than that of U–O. The Pa–O bond length of  $\text{PaO}_2(\text{H}_2\text{O})_5^+$  was calculated at 1.858 Å, which was 0.118 Å longer than that of  $\text{UO}_2(\text{H}_2\text{O})_5^{2+}$ . The Mulliken charges of the triply bonded oxygens ( $\text{O}_{\text{yl}}$ ) are  $-0.433$  and  $-0.160$  in  $\text{PaO}_2(\text{H}_2\text{O})_5^+$  and  $\text{UO}_2(\text{H}_2\text{O})_5^{2+}$  complexes, respectively. This result indicates that Pa–O triple bond of  $\text{PaO}_2(\text{H}_2\text{O})_5^+$  is weaker than that of U–O, because electrons are less donated from O to Pa than from O to U. This also acts on the optimized An–O bond lengths. The Pa–O bond length of  $\text{PaO}_2(\text{H}_2\text{O})_5^+$  is 0.059 Å longer than that of  $\text{PaO}(\text{H}_2\text{O})_6^{3+}$ . This result suggests that the addition of trans-oxygen to  $\text{PaO}(\text{H}_2\text{O})_6^{3+}$  destabilizes another monooxo Pa–O bond. In contrast, the U–O bond length is shortened from  $\text{UO}(\text{H}_2\text{O})_6^{4+}$  to  $\text{UO}_2(\text{H}_2\text{O})_5^{2+}$  by 0.022 Å. The cause of these differences will be cleared up by the Kohn–Sham orbital analysis in the next section.

**TABLE 2: Optimized An–O Bond Lengths (Å) and Mulliken Atomic Charges of Monooxo, Dioxo, and Monooxo Hydroxo Aquo Cations of Pa(V) and U(VI)<sup>a</sup>**

	$\text{PaO}(\text{H}_2\text{O})_6^{3+}$	$\text{PaO}(\text{OH})(\text{H}_2\text{O})_5^{2+}$	$\text{PaO}_2(\text{H}_2\text{O})_5^+$	$\text{UO}(\text{H}_2\text{O})_6^{4+}$	$\text{UO}(\text{OH})(\text{H}_2\text{O})_5^{3+}$	$\text{UO}_2(\text{H}_2\text{O})_5^{2+}$
Bond Lengths (Å)						
An– $\text{O}_{\text{yl}}$	1.799	1.816	1.858	1.718	1.720	1.740
An– $\text{O}_{\text{OH}}$		2.025		2.068	1.894	
An– $\text{O}_{\text{H}_2\text{O}}$ (equatorial)	2.487	2.534	2.593	2.382	2.432	2.494
An– $\text{O}_{\text{H}_2\text{O}}$ (axial)	2.422			2.286		
O–H		0.997			0.988	
Mulliken Charges						
An	2.076	2.028	1.659	2.044	2.028	1.690
$\text{O}_{\text{yl}}$	$-0.141$	$-0.255$	$-0.433$	0.047	$-0.039$	$-0.160$
$\text{O}_{\text{OH}}$	$-0.894$	$-0.854$	$(-0.433)$	$-0.817$	$-0.658$	$(-0.433)$
$\text{O}_{\text{H}_2\text{O}}$	$-0.923(\times 2)$	$-0.922$	$-0.942$	$-0.828(\times 2)$	$-0.880$	$-0.906$
(equatorial)	$-0.899(\times 2)$			$-0.862(\times 2)$		
	$-0.928$			$-0.871$		

<sup>a</sup> O–H bond lengths are also shown for monooxo hydroxo cations.

Table 1 also reveals another characteristic difference in the reaction energies between Pa(V) and U(VI) in aqueous solution. As the table shows, formulas 1–3 of Pa(V) system have less exothermic heats than those of U(VI) system. Especially, Pa(V) system gave a much less reaction heat energy for formula 3,  $-15$  kJ/mol, than the corresponding heat energy of U(VI) system,  $-189.27$  kJ/mol. This minor reaction heat of Pa(V) system indicates that  $\text{PaO}(\text{H}_2\text{O})_6^{3+}$  may coexist with  $\text{PaO}(\text{OH})(\text{H}_2\text{O})_5^{2+}$  as an equilibrium in strong acidic solution. In the present study, the equilibrium constant for hydrolytic reaction 3,  $K = [\text{PaO}(\text{H}_2\text{O})_6^{3+}][\text{H}_3\text{O}^+]/[\text{PaO}(\text{OH})(\text{H}_2\text{O})_5^{2+}]$ , cannot be determined, because it is hard to estimate the accurate Gibbs free energy change in such a hydrolytic reaction. However, this result obviously indicates that the coordinate bond of  $\text{OH}^-$  on  $\text{PaO}^{3+}$  is much weaker than that on  $\text{UO}^{4+}$ . This supports an experimental finding that  $\text{PaO}(\text{OH})^{2+}$  is the dominant chemical species in noncomplexing acidic solutions such as  $\text{HClO}_4$ . It is interesting to note that according to Le Naoul et al.,  $\text{OH}^-$  of  $\text{PaO}(\text{OH})(\text{H}_2\text{O})_5^{2+}$  is easily replaced by another complexing ligand such as  $\text{SO}_4^{2-}$ . In contrast,  $\text{UO}(\text{OH})(\text{H}_2\text{O})_5^{3+}$  is not a stable chemical species even in highly concentrated ligand solutions. Actually, a stable dioxo cation is spontaneously produced for U(VI).

For the formation of monooxo cations, Table 1 shows that the reaction heats are  $-209.28$  kJ/mol and  $-598.24$  kJ/mol for Pa(V) and U(VI), respectively. Therefore, the present calculation supports the experimental observation that both these monooxo cations were spontaneously produced. However, this also indicates that the Pa(V) monooxo cation is much less stable than the U(VI) one. As shown in Table 2,  $\text{PaO}(\text{H}_2\text{O})_6^{3+}$  and  $\text{UO}(\text{H}_2\text{O})_6^{4+}$  gave quite different Mulliken charges for O atom in An–O bonds:  $-0.141$  and  $+0.047$ , respectively. Due to this small electron donation, it is presumed that Pa(V) may give a much weaker Pa–O bond than the U–O bond. This may cause the dissociation of Pa–O bond under a highly concentrated coordinating ligand condition. Actually, Le Naour et al. found that Pa(V) formed heptafluoro complex,  $\text{PaF}_7^{2-}$ , in 13 M HF solution, although U(VI) kept the dioxo cation in the same solution.

**Instability of Dioxo Pa(V) Species from Orbital Point of View.** To reveal the reason for the instability of Pa(V) dioxo cation, electronic structures and An–O bonding properties are compared for Pa(V) and U(VI) cations in this section. For investigating the difference in the dioxo cation formations, we first calculated the electronic properties of bare cations:  $\text{PaO}^{3+}$ ,  $\text{UO}^{4+}$ ,  $\text{PaO}(\text{OH})^{2+}$ ,  $\text{UO}(\text{OH})^{3+}$ ,  $\text{PaO}_2^{2+}$ , and  $\text{UO}_2^{2+}$ . Calculated several highest-occupied Kohn–Sham orbitals and their energies



**TABLE 3: Calculated Kohn–Sham Orbitals and Their Energies (au) of Bare Monooxo, Dioxo, and Monooxo Hydroxo Cations of Pa(V) and U(VI) Cations for Several Highest Occupied Orbitals<sup>a</sup>**

PaO <sup>3+</sup>				UO <sup>4+</sup>		
	sym	energy	character	sym	energy	character
HOMO	a <sub>1</sub> (σ)	−1.083	5f <sub>z(5z<sup>2</sup>−3r<sup>2</sup>)</sub> , 6d <sub>z<sup>2</sup></sub> , 7s + 2p <sub>z</sub> (O <sub>yl</sub> )	a <sub>1</sub> (σ)	−1.647	5f <sub>z(5z<sup>2</sup>−3r<sup>2</sup>)</sub> , 6d <sub>z<sup>2</sup></sub> , 7s, 7p <sub>z</sub> + 2p <sub>z</sub> (O <sub>yl</sub> )
HOMO-1	b <sub>2</sub> (π)	−1.089	5f <sub>y(5z<sup>2</sup>−r<sup>2</sup>)</sub> , 6d <sub>yz</sub> + 2p <sub>y</sub> (O <sub>yl</sub> )	b <sub>2</sub> (π)	−1.674	5f <sub>y(5z<sup>2</sup>−r<sup>2</sup>)</sub> + 2p <sub>y</sub> (O <sub>yl</sub> )
HOMO-2	b <sub>1</sub> (π)	−1.091	5f <sub>x(5z<sup>2</sup>−r<sup>2</sup>)</sub> , 6d <sub>xz</sub> + 2p <sub>x</sub> (O <sub>yl</sub> )	b <sub>1</sub> (π)	−1.674	5f <sub>x(5z<sup>2</sup>−r<sup>2</sup>)</sub> + 2p <sub>x</sub>
PaO <sub>2</sub> <sup>+</sup>				UO <sub>2</sub> <sup>2+</sup>		
	sym	energy	character	sym	energy	character
HOMO	(σ <sub>g</sub> )	−0.660	6d <sub>z<sup>2</sup></sub> , 7s + 2p <sub>z</sub>	(σ <sub>u</sub> )	−0.969	5f <sub>z(5z<sup>2</sup>−3r<sup>2</sup>)</sub> , 7p <sub>z</sub> + 2p <sub>z</sub>
HOMO-1	(π <sub>g</sub> )	−0.669	6d <sub>xz</sub> + 2p <sub>x</sub>	(σ <sub>g</sub> )	−0.981	6d <sub>z<sup>2</sup></sub> , 7s + 2p <sub>z</sub>
HOMO-2	(π <sub>g</sub> )	−0.669	6d <sub>yz</sub> + 2p <sub>y</sub>	(π <sub>u</sub> )	−1.008	5f <sub>x(5z<sup>2</sup>−r<sup>2</sup>)</sub> , 5f <sub>y(5z<sup>2</sup>−r<sup>2</sup>)</sub> , 7p <sub>x</sub> , 7p <sub>y</sub> + 2p <sub>x</sub> , 2p <sub>y</sub>
HOMO-3	(σ <sub>u</sub> )	−0.706	5f <sub>z(5z<sup>2</sup>−3r<sup>2</sup>)</sub> , 7p <sub>z</sub> + 2p <sub>z</sub>	(π <sub>u</sub> )	−1.008	5f <sub>x(5z<sup>2</sup>−r<sup>2</sup>)</sub> , 5f <sub>y(5z<sup>2</sup>−r<sup>2</sup>)</sub> , 7p <sub>x</sub> , 7p <sub>y</sub> + 2p <sub>x</sub> , 2p <sub>y</sub>
HOMO-4	(π <sub>u</sub> )	−0.709	5f <sub>x(5z<sup>2</sup>−r<sup>2</sup>)</sub> , 7p <sub>x</sub> + 2p <sub>x</sub>	(π <sub>g</sub> )	−1.019	6d <sub>yz</sub> + 2p <sub>y</sub>
HOMO-5	(π <sub>u</sub> )	−0.709	5f <sub>y(5z<sup>2</sup>−r<sup>2</sup>)</sub> , 6d <sub>yz</sub> , 7p <sub>y</sub> + 2p <sub>y</sub>	(π <sub>g</sub> )	−1.019	6d <sub>xz</sub> + 2p <sub>y</sub>
PaO(OH) <sup>2+</sup>				UO(OH) <sup>3+</sup>		
	sym	energy	character	sym	energy	character
HOMO	a <sub>1</sub> (σ <sup>+</sup> )	−0.568	5f <sub>z(5z<sup>2</sup>−3r<sup>2</sup>)</sub> , 6d <sub>z<sup>2</sup></sub> + 2p <sub>z</sub> (O <sub>yl</sub> )	a <sub>1</sub> (σ <sup>+</sup> )	−1.226	5f <sub>z(5z<sup>2</sup>−3r<sup>2</sup>)</sub> , 6d <sub>z<sup>2</sup></sub> , 7s, 7p <sub>z</sub> + 2p <sub>z</sub> (O <sub>yl</sub> )
HOMO-1	b <sub>2</sub> (π)	−0.573	5f <sub>y(5z<sup>2</sup>−r<sup>2</sup>)</sub> , 6d <sub>yz</sub> , 7p <sub>y</sub> + 2p <sub>y</sub> (O <sub>yl</sub> )	b <sub>2</sub> (π)	−1.263	5f <sub>y(5z<sup>2</sup>−r<sup>2</sup>)</sub> , 7p <sub>y</sub> + 2p <sub>y</sub> (O <sub>yl</sub> , OH)
HOMO-2	b <sub>1</sub> (π)	−0.573	5f <sub>x(5z<sup>2</sup>−r<sup>2</sup>)</sub> , 6d <sub>xz</sub> , 7p <sub>x</sub> + 2p <sub>x</sub> (O <sub>yl</sub> )	b <sub>1</sub> (π)	−1.263	5f <sub>x(5z<sup>2</sup>−r<sup>2</sup>)</sub> , 7p <sub>x</sub> + 2p <sub>x</sub> (O <sub>yl</sub> , OH)
HOMO-3	b <sub>2</sub> (π)	−0.607	5f <sub>y(5z<sup>2</sup>−r<sup>2</sup>)</sub> , 6d <sub>yz</sub> , 7p <sub>y</sub> + 2p <sub>y</sub> (OH)	b <sub>2</sub> (π)	−1.266	6d <sub>yz</sub> + 2p <sub>y</sub> (O <sub>yl</sub> , OH)
HOMO-4	b <sub>1</sub> (π)	−0.607	5f <sub>x(5z<sup>2</sup>−r<sup>2</sup>)</sub> , 6d <sub>xz</sub> , 7p <sub>x</sub> + 2p <sub>x</sub> (OH)	b <sub>1</sub> (π)	−1.266	6d <sub>xz</sub> + 2p <sub>x</sub> (O <sub>yl</sub> , OH)
HOMO-5	a <sub>1</sub> (σ <sup>+</sup> )	−0.610	5f <sub>z(5z<sup>2</sup>−3r<sup>2</sup>)</sub> , 7d <sub>z<sup>2</sup></sub> , 7s + 2p <sub>z</sub> (OH), 1s(OH)	a <sub>1</sub> (σ <sup>+</sup> )	−1.339	5f <sub>z(5z<sup>2</sup>−3r<sup>2</sup>)</sub> , 7d <sub>z<sup>2</sup></sub> , 7s + 2p <sub>z</sub> (OH), 1s(OH)

<sup>a</sup> LC-BOP functional was used in Kohn–Sham calculations.

are displayed in Table 3. These orbitals are drawn in Figure 2. It should be noted that we used LC-BOP results in the orbital analyses. This is because long-range exchange interaction essentially contributes to the stabilization of occupied  $\pi$  orbitals in comparison to  $\sigma$  orbitals. This indicates that the long-range exchange may be necessary to discuss molecular orbitals quantitatively in DFT calculations. In the present calculation, we found no obvious differences between LC-BOP and B3LYP orbital diagrams including orbital energies and structures, despite of the clear differences between LC-BOP and BLYP results. Since B3LYP partly contains long-range exchange interactions, this indicates that there is a small but certain long-range exchange effect on these orbitals. As shown in Table 3, the chemical bonds of both PaO<sup>3+</sup> and UO<sup>4+</sup> ions consist of one  $\sigma$  orbital (a<sub>1</sub>: HOMO) and two  $\pi$  orbitals (b<sub>1</sub> and b<sub>2</sub>: HOMO-1 and HOMO-2). The major difference between these bonds was found in the constituent atomic orbitals: although two  $\pi$  bonds consist of two 5f orbitals of U with 2p orbitals of O in UO<sup>4+</sup>, 5f and 6d orbitals of Pa compose these  $\pi$  bonds in PaO<sup>3+</sup>. We presume that the U–O bond of UO<sup>4+</sup> is a typical triple bond, and PaO<sup>3+</sup> uses 6d orbital in place of 5f orbital to form the Pa–O triple bond. This may suggest that the weakness of the Pa–O bond is attributable to the lack of one 5f orbital constructing the triple bond.

The detailed analysis of calculated An–O triple bonding orbitals gives further information on the relative stability of the dioxo cations. The  $\pi$  bonds of PaO<sup>3+</sup> (b<sub>1</sub>: HOMO-2) consist of 5f<sub>x(5z<sup>2</sup>−r<sup>2</sup>)</sub> (and therefore 5f<sub>y(5z<sup>2</sup>−r<sup>2</sup>)</sub> for another degenerated  $\pi$  orbital, HOMO-1), 6d<sub>xz</sub> (6d<sub>yz</sub>), and 7p<sub>x</sub> (7p<sub>y</sub>) orbitals of Pa atom

with 2p<sub>x</sub> orbital of O atom. In cases where O coordinates to the trans position of PaO<sup>3+</sup>, the 2p<sub>x</sub> orbital of trans-O atom forms a bonding orbital with the 5f<sub>x(5z<sup>2</sup>−r<sup>2</sup>)</sub> orbital, as seen in Figure 3. However, it also constructs the antibonding orbital with the 6d<sub>xz</sub> orbital, and this antibonding orbital destabilizes the dioxo formation of Pa(V). Similar problems have been seen in several transition metal oxocation systems. For instance, tetravalent vanadium V(IV), which has d<sup>0</sup> electron configuration, usually forms no dioxo cations. This is due to the antibonding 6d<sub>xz</sub>-2p and 6d<sub>yz</sub>-2p orbitals of the dioxo cation in analogy with that of Pa(V). On the other hand, experiments have suggested that stable dioxo cations are produced for several cations containing d<sup>0</sup> configuration, e.g. pentavalent vanadium, hexavalent molybdenum, and hexavalent tungsten cations. However, cis-type bended structures are produced for these cations, because antibonding d<sub>xz</sub>-2p<sub>x</sub> orbital interrupts the trans-O coordination to monooxo cations. It should be noted that no cis-type bended structure is given for Pa(V) in aqueous solution. Even though the second O atom approaches the cis position (+x direction), the 2d<sub>y</sub> orbital indeed forms a bonding orbital with 6d<sub>xz</sub> orbital. However, the 5f<sub>x(5z<sup>2</sup>−r<sup>2</sup>)</sub> orbital forms no  $\pi$  bondings with the 2d<sub>y</sub> orbital of cis-O atom in turn, because 5f<sub>x(5z<sup>2</sup>−r<sup>2</sup>)</sub> has no node in the y direction. It is, therefore, presumed that the trans dioxo structure is more stable than the cis one, despite the energy loss from the 6d<sub>xz</sub>-2p<sub>x</sub> (6d<sub>yz</sub>-2p<sub>y</sub>) antibonding orbitals is larger than the energy gain from the 5f<sub>x(5z<sup>2</sup>−r<sup>2</sup>)</sub>-6d<sub>x</sub> (5f<sub>y(5z<sup>2</sup>−r<sup>2</sup>)</sub>-6d<sub>y</sub>) hybridization. Actually, the present DFT calculations also gave no cis-type structures for PaO<sub>2</sub><sup>+</sup>. It is interesting to note that trans-type dioxo cations are produced for Re(V) and Os(VI) containing d<sup>2</sup>

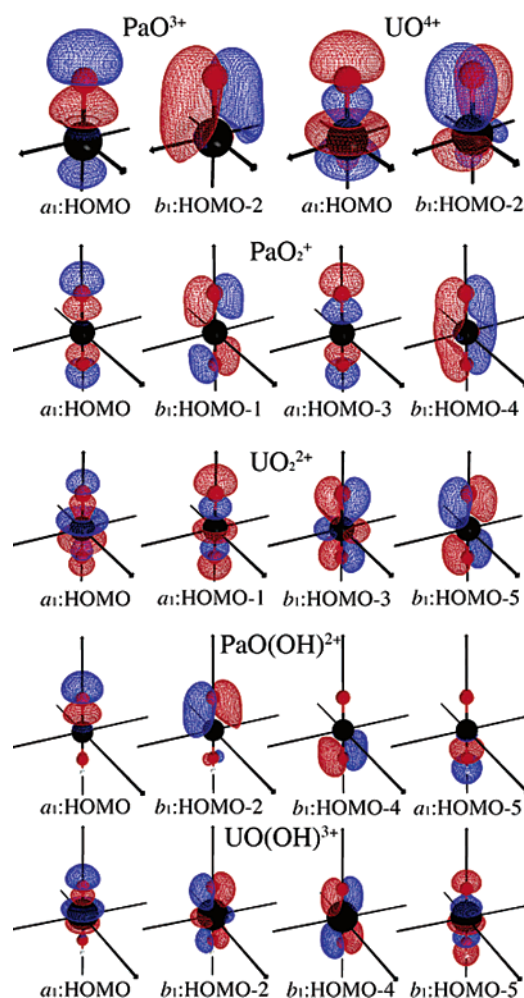


**Figure 2.** Calculated Kohn–Sham orbitals of bare monooxo, dioxo, and monooxo hydroxo cations of Pa(V) and U(VI) for several orbitals chiefly contributing to chemical bonds. LC-BOP functional was used in Kohn–Sham calculations.

electronic configuration. In these dioxo cations, the energy loss from antibonding  $6d-2p$  orbitals is recovered by the energy gain from the stabilization of two localized  $6d$  electrons.<sup>28</sup> This stabilization energy from  $6d$  orbitals is not given for Pa(V), because Pa(V) has no occupied  $6d$  orbitals in electronic structure.

We should notice that the order of the Kohn–Sham orbitals is different from that of Santos et al. On the basis of the Hartree–Fock (HF) calculation, Santos et al.<sup>29</sup> concluded that HOMO of  $\text{PaO}_2^+$  is  $\sigma_u$  orbital, which is followed at modest intervals by  $\pi_u$ ,  $\sigma_g$ , and  $\pi_g$  orbitals. In contrast, the present calculation with any exchange–correlation functional showed that HOMO is  $\sigma_g$  orbital, which is followed by  $\pi_g$ ,  $\sigma_u$ , and  $\pi_u$  orbitals. This difference is due to the level of calculations. Although the HF orbitals were calculated with no electron correlation, Kohn–Sham orbitals were given with an electron correlation in exchange–correlation functional. In case where orbitals are lying in very narrow energy region, the discrepancy in the order of orbital energies is often found in HF and DFT calculations. However, this discrepancy gave no problems in the present study, because we discuss not the energy level but the constitution of atomic orbitals.

On the other hand, calculated Kohn–Sham orbitals clearly showed the stable U–O triple bonds of  $\text{UO}_2^{2+}$ . In Table 3, it was found that no  $6d$  orbitals participate in two  $\pi$  bonds in  $\text{UO}^{4+}$

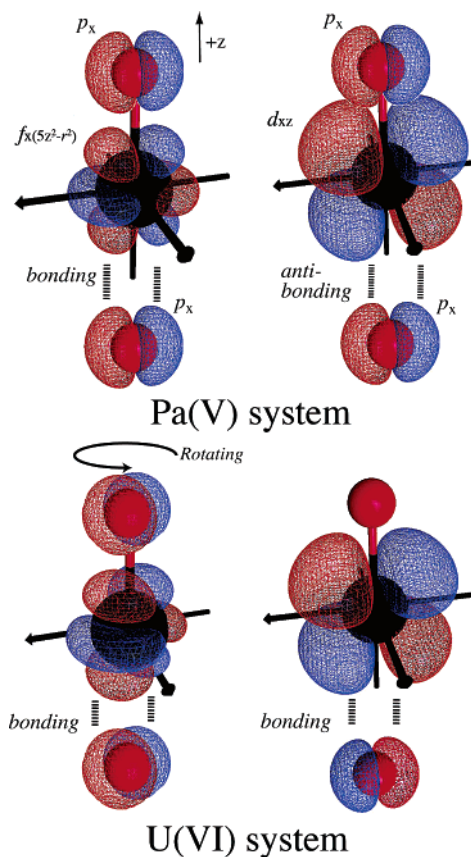


**Figure 3.** Conceptual diagram of the bonding and antibonding dioxo formation of Pa(V) and U(VI) cations. The triple bond in  $\text{PaO}^{3+}$  consists of one  $\sigma$  and two  $\pi$  bonds, in which two  $\pi$  orbitals are the hybridization of  $5f_{x(5z^2-r^2)}$  and  $6d_{xz}$  orbitals with  $2p_x$  orbital. The addition of O to  $\text{PaO}^{3+}$  from the trans position forms bonding  $5f_{xz}-2p_x$  and antibonding  $7d_{xz}-2p_x$  orbitals. This antibonding orbital was not found in  $\text{UO}_2^{2+}$ , because  $\pi$  bonds in this dioxo cation consist of the angled  $5f_{x(5z^2-r^2)}$  and  $5f_{y(5z^2-r^2)}$  and  $2p_x+2p_y$  orbitals with no  $6d_{xz}$  orbitals.

(cf. HOMO-1 and HOMO-2 in Table 3) in contrast to  $\text{PaO}^{3+}$ . The  $6d_{xz}$  and  $6d_{yz}$  orbitals, in turn, formed the  $\pi$  bonds in  $\text{UO}_2^{2+}$ . However, we found that the antibonding  $6d_{xz}-2p_x$  ( $6d_{yz}-2p_y$ ) orbital does not counteract the bonding  $5f-2p$  orbital in  $\text{UO}_2^{2+}$  system. As we can see from Table 3 and Figure 2, although  $6d_{xz}$  and  $6d_{yz}$  orbitals form two  $\pi_u$  bonds with  $2p_x$  or  $2p_y$  orbitals of trans-O atom, the  $\pi_g$  bonds of U–O bond species obtained from no symmetry constraint calculations are at an angle with these  $\pi_u$  bonds in terms of the principal  $z$ -axis in  $\text{UO}_2^{2+}$  (cf. HOMO-3 and HOMO-5 of  $\text{UO}_2^{2+}$  in Figure 1). The constituting atomic orbitals of  $\pi_g$  orbitals are the linear combination of two  $E_u$  atomic orbitals: the  $5f_{x(5z^2-r^2)} + 5f_{y(5z^2-r^2)}$  and  $7p_x+7p_y$  ( $7p_x-7p_y$ ) orbitals of U(VI) ion with  $2p_x+2p_y$  ( $2p_x-2p_y$ ) of trans-O atom. This makes a great effort to the formation of the stable dioxo cation. As shown in Figure 3, the formation of the  $\pi_g$  bonds,  $6d_{xz}$  ( $6d_{yz}$ ) –  $2p_x$  ( $2p_y$ ) of trans O atoms, hardly affects the antibonding  $\pi_u$  bonds of  $f_{x(5z^2-r^2)}$  ( $f_{y(5z^2-r^2)}$ ) –  $2p_x$  ( $2p_y$ ). Although we identified no precise reasons for the angle of  $\pi_g$  and  $\pi_u$  orbitals, we found an important point for understanding the reason. Table 4 lists the optimized angles of  $\pi_g$  and  $\pi_u$  orbitals for various methods. As we can see from the table, HF method provided  $0.035\pi$  for this angle, which is much smaller than those obtained in DFT calculations. This may indicate that this angle is significantly affected by electron correlation. The stability of the  $\text{UO}_2^{2+}$  triple bond was also supported by the Kohn–Sham orbitals of the singly deprotonated dioxo cation,  $\text{UO(OH)}^{3+}$ , having similar bonds to  $\text{UO}_2^{2+}$ : six highest oc-

**TABLE 4: Relative Angle of  $\pi_g$  Orbitals of  $\text{UO}_2^{2+}$  from Its  $\pi_u$  Orbital<sup>a</sup>**

functional	LC-BOP	B3LYP	BLYP	SVWN	HF
relative angle	0.203 $\pi$	0.207 $\pi$	0.094 $\pi$	0.220 $\pi$	0.035 $\pi$

<sup>a</sup> The values are the angles between constituent  $2p_x$  and  $2p_y$  orbitals of  $\pi_u$  orbitals.

cupied orbitals contribute to two triple bonds of U and two trans O atoms. Comparing HOMOs of  $\text{UO}(\text{OH})^{3+}$  and  $\text{UO}_2^{2+}$ , it was found that the HOMO ( $\sigma_u$ ) of  $\text{UO}_2^{2+}$  is stiffened by the dissociation of  $\text{H}^+$ , while all the other five orbitals are conserved. It is presumed that this caused the reaction 4 exothermic.

We still have one question remaining: why is the 6d contribution stronger in  $\pi$  bonds of  $\text{PaO}^{3+}$  than in those of  $\text{UO}_2^{2+}$ , despite the same number of electrons are contained in Pa(V) and U(VI) cations? We guess that this may be due to the energy levels of 6d orbitals compared to those of 5f orbitals. From the context of actinide contraction, it is known that the nuclear charge of Pa ( $Z = 91$ ) is more shielded by inner-shell electrons than that of U ( $Z = 92$ ). This leads to the destabilization of 5f orbitals in Pa as compared to those in U. We suppose that 5f electrons of Pa(V) complexes, which are donated from coordinating atoms, are energetically less stable than 6d electrons.<sup>1,30</sup> This argument is supported by a previous detailed work on actinyl systems.<sup>31</sup> For  $\text{PaO}^{3+}$ , the Pa–O bond, therefore, consists of considerable 6d–2p orbitals besides 5f–2p orbitals. This argument is also supported by calculated virtual orbital energies of bare  $\text{Pa}^{5+}$  and  $\text{U}^{6+}$  cations. Calculated results showed that  $\text{Pa}^{5+}$  contains virtual orbitals in the energetic order of 7p, 7s, 6d, and 5f from LUMO to LUMO+3, while the virtual orbitals of  $\text{U}^{6+}$  are in the order of 5f, 6d, 7s, and 7p. These energetic orders may cause the inclusion of 6d–2p orbitals in the bonds of  $\text{PaO}^{3+}$ . This argument is also applicable to the difference in the bonding properties of three isoelectric early actinide cations: tetravalent thorium Th(IV), Pa(V) and U(VI). It is widely accepted that Th(IV) cation forms no chemical bonds probably due to the nonparticipation of 5f orbitals in bonds. By calculating bare  $\text{Th}^{4+}$  and  $\text{Pa}^{5+}$  cations, we actually found that the virtual 5f orbital energies of  $\text{Th}^{4+}$  are much higher than even those of  $\text{Pa}^{5+}$ . It is known that protactinium is the lightest actinide involving 5f orbitals in chemical bonds, and the chemical bonds of uranium are usually dominated by 5f orbitals. Hence, we conclude that the energetic order of 5f and 6d orbitals may have serious effect on the bonding characters of mono and dioxo cations of Pa(V) and U(VI).

#### 4. Conclusions

In summary, the present calculations clearly revealed the difference in the oxidizations of Pa(V) and U(VI) cations in aqueous solution as the follows: The  $6d_{xz}$  and  $6d_{yz}$  orbitals contributed even to the  $\text{PaO}^{3+}$  bond as contrasted to the  $\text{UO}^{4+}$  bond consisting of only the 5f orbital. This may come from the difference in the energetic orders of 5f and 6d orbitals. For  $\text{PaO}_2^{2+}$ , these  $6d_{xz}$  and  $6d_{yz}$  orbitals formed the antibonding orbitals with the 2p orbitals of O, and destabilized the trans-O coordination. In contrast, the trans-O coordination of  $\text{UO}_2^{2+}$  was stabilized by the  $5f_{x(5z^2-r^2)}$  and  $5f_{y(5z^2-r^2)}$  orbitals, because these orbitals produced the bonding orbital with the 2p orbital. In  $\text{UO}_2^{2+}$ , bonding 5f–2p orbitals coexisted at an angle with the 6d–2p orbitals as opposed to  $\text{PaO}_2^{2+}$ . The  $\pi_g$  and  $\pi_u$  orbitals of the triple bond were, consequently, deployed on the different plane in  $\text{UO}_2^{2+}$ . We found that this is due to an electron correlation.

**Acknowledgment.** We would like to thank Dr. Christoph Hennig at ROBL for providing us experimental data and lots of fruitful discussions. This research was supported in part by a Grant-in-Aids for Scientific Research (A) and (C). This research was also supported in part by CREST (Core Research for Evolutional Science and Technology) of Japan Science and Technology Corporation (JST) and by a contribution from Hitachi Chemical Co., Ltd.

**Supporting Information Available:** Coordination geometries and Mulliken atomic charges of bare cations obtained by LC-BOP functional (Table S1) This material is available free of charge via the Internet at <http://pubs.acs.org>.

#### References and Notes

- (1) Katz, J. J.; Seaborg, G. In *The Chemistry of the actinide elements*; Chapman and Hall: New York, 1986.
- (2) Benedict, M.; Pigford, T. H.; Levi, H. W. In *Nuclear Chemical Engineering*, 2nd ed.; McGraw-Hill Series in Nuclear Engineering, McGraw-Hill: 1981.
- (3) Choppin, G. R.; Rydberg, J.; Liljenzin, J.-O. In *Radiochemistry and Nuclear Chemistry*, 3rd ed.; Butterworth-Heinemann: 2001.
- (4) Welch, G. A. *Nature* **1953**, 172, 458.
- (5) Guillaumont, R.; Bouissieres, G.; Muxart, R. *Actinides Rev.* **1968**, 1, 135.
- (6) Brown, D.; Maddock, A. G. *Quart. Rev.* **1963**, XVII (3), 289.
- (7) Le Naour, C.; Trubert, D.; Di Giandomenico, V. Di.; Fillaux, C.; Den Auwer, C.; Moisy, P.; Hennig, C. *Inorg. Chem.* **2005**, 44, 9542–9546.
- (8) Keller, O. L., Jr. *Inorg. Chem.* **1963**, 2, 783.
- (9) Japan Nuclear Cycle Development Institute (JNC). *H12: Project to Establish the Scientific and Technical Basis for HLW Disposal in Japan*; 1999.
- (10) Becke, A. D. *J. Chem. Phys.* **1993**, 98, 5648.
- (11) Lee, C.; Yang, W.; Parr, R. G. *Phys. Rev. B* **1988**, 37, 785.
- (12) Frisch, M. J.; Trucks, G. W.; Schlegel, H. B.; Scuseria, G. E.; Robb, M. A.; Cheeseman, J. R.; Montgomery, J. A., Jr.; Vreven, T.; Kudin, K. N.; Burant, J. C.; Millam, J. M.; Iyengar, S. S.; Tomasi, J.; Barone, V.; Mennucci, B.; Cossi, M.; Scalmani, G.; Rega, N.; Petersson, G. A.; Nakatsuji, H.; Hada, M.; Ehara, M.; Toyota, K.; Fukuda, R.; Hasegawa, J.; Ishida, M.; Nakajima, T.; Honda, Y.; Kitao, O.; Nakai, H.; Klene, M.; Li, X.; Knox, J. E.; Hratchian, H. P.; Cross, J. B.; Bakken, V.; Adamo, C.; Jaramillo, J.; Gomperts, R.; Stratmann, R. E.; Yazyev, O.; Austin, A. J.; Cammi, R.; Pomelli, C.; Ochterski, J. W.; Ayala, P. Y.; Morokuma, K.; Voth, G. A.; Salvador, P.; Dannenberg, J. J.; Zakrzewski, V. G.; Dapprich, S.; Daniels, A. D.; Strain, M. C.; Farkas, O.; Malick, D. K.; Rabuck, A. D.; Raghavachari, K.; Foresman, J. B.; Ortiz, J. V.; Cui, Q.; Baboul, A. G.; Clifford, S.; Cioslowski, J.; Stefanov, B. B.; Liu, G.; Liashenko, A.; Piskorz, P.; Komaromi, I.; Martin, R. L.; Fox, D. J.; Keith, T.; Al-Laham, M. A.; Peng, C. Y.; Nanayakkara, A.; Challacombe, M.; Gill, P. M. W.; Johnson, B.; Chen, W.; Wong, M. W.; Gonzalez, C.; Pople, J. A. *Gaussian 03, revision C.02*; Gaussian, Inc.: Wallingford, CT, 2004.
- (13) (a) Hay, P. J.; Martin, R. L. *J. Chem. Phys.* **1998**, 109, 3875. (b) Schreckenbach, G.; Hay, P. J.; Martin, R. L. *J. Comput. Chem.* **1999**, 20, 70. (c) Hay, P. J.; Martin, R. L.; Schreckenbach, G. *J. Phys. Chem. A* **2000**, 104, 6259. (d) Vallet, V.; Wahlgren, U.; Schimmelpfennig, B.; Moll, H.; Szabo, Z.; Grenthe, I. *Inorg. Chem.* **2001**, 40, 3516.
- (14) (a) Barone, V.; Cossi, M. *J. Phys. Chem. A* **1998**, 102, 1995. (b) Cossi, M.; Rega, N.; Scalmani, G.; Barone, V. *J. Comput. Chem.* **2003**, 24, 669. (c) Miertys, S.; Scrocco, E.; Tomasi, J. *J. Chem. Phys.* **1981**, 55, 117.
- (15) Cancès, E.; Mennucci, B.; Tomasi, J. *J. Chem. Phys.* **1997**, 107, 3032.
- (16) Kohn, W.; Sham, L. J. *Phys. Rev.* **1965**, 140, A1133.
- (17) Vosko, S. H.; Wilk, L.; Nusair, M. *Can. J. Chem.* **1980**, 58, 1200.
- (18) Becke, A. D. *Phys. Rev. A* **1988**, 38, 3098–3100.
- (19) Ikura, H.; Tsuneda, T.; Yanai, T.; Hirao, K. *J. Chem. Phys.* **2001**, 115, 9975–9999.
- (20) Tsuneda, T.; Suzumura, T.; Hirao, K. *J. Chem. Phys.* **1999**, 110, 10664–10678.
- (21) Schmidt, M. W.; Baldridge, K. K.; Boatz, J. A.; Elbert, S. T.; Gordon, M. S.; Jensen, J. H.; Koseki, S.; Matsunaga, N.; Nguyen, K. A.; Su, S. J.; Windus, T. L.; Dupuis, M.; Montgomery, J. A. General Atomic and Molecular Electronic Structure System: GAMESS v. 22. *J. Comput. Chem.* **1993**, 14, 1347–1363.
- (22) Dorg, M.; Stoll, H.; Preuss, H.; Pitzer, R. M. *J. Phys. Chem.* **1993**, 97, 5852.
- (23) Bergner, A.; Dolg, M.; Kuchle, W.; Stoll, H.; Preuss, H. *J. Mol. Phys.* **1993**, 80, 1431.
- (24) Huzinaga, S. *J. Chem. Phys.* **1965**, 42, 1293.

- (24) Dunning, T. H., Jr. *J. Chem. Phys.* **1989**, 90, 1007.
- (25) Bode, B. M.; Gordon, M. S. *J. Mol. Graphics Modell.* **1998**, 16, 133–138.
- (26) (a) Combes, J.-M.; Chisholm-Brause, C. J.; Brown, G. E., Jr.; Parks, G. A.; Conradson, S. D.; Eller, P. G.; Triay, I. R.; Hobart, D. E.; Meijer, A. *Environ. Sci. Technol.* **1992**, 26, 376. (b) Allen, P. G.; Bucher, J. J.; Shuh, D. K.; Edelstein, N. M.; Reich, T. *Inorg. Chem.* **1997**, 36, 4676. (c) Conradson, S. D. *Appl. Spectrosc.* **1998**, 52, 252A. (d) Wahlgren, U.; Moll, H.; Grenthe, I.; Schimmelpfennig, B.; Maron, L.; Vallet, V.; Gropen, O. *J. Phys. Chem. A* **1999**, 103, 8257.
- (27) Tsushima, S.; Yang, T.; Mochizuki, Y.; Okamoto, Y. *Chem. Phys. Lett.* **2003**, 375, 204.
- (28) Shriver, D. F.; Atkins, P. W. In *Inorganic Chemistry*; 3rd ed.; W. H. Freeman & Company: 1999.
- (29) Straka, M.; Dylla, K. G.; Pykkö, P. *Theor. Chem. Acc.* **2001**, 106, 393.
- (30) Cotton, S. In *Lanthanides and Actinides*; Oxford University Press: New York, 1991.
- (31) Santos, M.; Pires de Matos, A.; Marçalo, J.; Gibson, J. K.; Haire, R. G.; Tyagi, R.; Pitzer, R. M. *J. Phys. Chem. A* **2006**, 110, 5751.